Effect of Solvent Precipitation on the Crystallization Behavior and Morphology of Nylon 6,6

JOAN T. MUELLERLEILE* and JOHN J. FREEMAN

Analytical Sciences Center, Monsanto Corporate Research, 700 Chesterfield Parkway North, St. Louis, Missouri 63198

SYNOPSIS

This work describes the effect of solvent precipitation on the crystallization behavior and morphology of nylon 6,6. We found that solvent precipitation of nylon 6,6 induces elevated crystallization temperatures upon cooling from the melt (T_{mc}) and highly nucleated morphologies that rival those induced by rapid, thermal reprocessing such as melt reextrusion or heterogeneous nucleating agents such as CaF_2. The primary techniques used to characterize these changes in crystallization behavior and morphology were differential scanning calorimetry (DSC), polarized optical microscopy (POM), and wide-angle X-ray scattering (WAXS). Several other supplementary techniques were employed for identifying the origin of the crystallization behavior and morphological changes after solvent precipitation. Our results are consistent with the hypothesis in which dissolved nylon reorients to form ordered H-bonded regions that later serve as nucleation sites during melt processing. Finally, T_{mc} decreased with nylon 6,6 solution concentration prior to precipitation. These results suggest that polymer entanglements in solution also affect the crystallization behavior and morphology of the solvent-precipitated nylon 6,6. © 1994 John Wiley & Sons, Inc.

INTRODUCTION

As part of our investigation of factors affecting nylon 6,6 morphology, rapid solvent precipitation by adding a nonsolvent was originally used to simply purify the commercial nylon 6,6 pellets. Subsequent analysis of the solvent-precipitated nylon 6,6 revealed crystallization behavior and morphology rivaling those induced by either thermal processing or heterogeneous nucleation. While the latter two processes are commonly employed to control the morphology of semicrystalline polymers,[1-8] there have been only a few reports in the literature describing the role of solvent precipitation for inducing similar effects. Khanna and co-workers described the effects of rapid solvent precipitation on nylon crystallization and morphology, with passing reference to this effect for nylon 6,6. They hypothesized that while in solution, hydrogen-bonded disorder in the virgin melt is disrupted and ordered hydrogen-bonded regions are formed. Following precipitation, these ordered regions in the precipitated nylon persist in the subsequent melt and therefore influence its crystallization behavior and morphology.[9-12]

Our goal was to more fully understand the magnitude and mechanism by which solvent precipitation alters crystallization behavior and morphology of nylon 6,6. The work described in this study involved producing solvent-precipitated nylon 6,6 from several nylon 6,6 solvent–nonsolvent combinations. The crystallization behavior and morphology of the samples were characterized and compared with those for reextruded or heterogeneously nucleated nylon 6,6. Additional characterization techniques were conducted to clarify the possible mechanisms associated with the effect of solvent precipitation on the crystallization behavior and morphology of nylon 6,6.

EXPERIMENTAL

Sample Preparation

Commercial-grade melt-polymerized nylon 6,6 pellets were kindly provided by J. C. Middleton and

* To whom correspondence should be addressed. Current address: Owens-Corning Technical Center, 2790 Granville Road, Route 16, Granville, Ohio 43023.

Journal of Applied Polymer Science, Vol. 54, 135–152 (1994)
 CCC 0021-8995/94/020135-18

O. J. Parker (Monsanto Company, Chemical Group). The sample was utilized as received. Solvent-precipitated nylon 6,6 samples were prepared as follows:

1. Trifluoroethanol-precipitated nylon 6,6 (TFE nylon 6,6) was prepared by adding 0.2–0.3 g nylon 6,6 pellets in 15–20 mL of TFE (Eastman-Kodak, 99% purity). To accelerate the dissolution process, the mixture was placed in a vacuum oven at ambient pressure and heated to 55–60°C for a time ranging from several hours to overnight, depending on how readily the polymer dissolved in the TFE. The nylon 6,6 was *rapidly* precipitated by adding the nylon 6,6/TFE solution with vigorous stirring to methanol (MeOH) (Fisher Scientific, Optima grade; MeOH–TFE volume ca. 10 : 1). The solid was filtered using a Millipore type FG 0.2-μm Fluoropore filter. The precipitate was a fine white powder. Several nylon 6,6 concentrations were prepared, ranging from 0.1 to 5% by weight. The material was filtered and dried under vacuum at ca. 45–55°C. The final sample was in the form of small chunks several millimeters in diameter.
2. A second type of TFE nylon 6,6 was also prepared in the exact same fashion as described above, except that the solution was precipitated in the nonsolvent diethyl ether (DEE) (Mallinckrodt, 99% purity) instead of MeOH. The sample was filtered as described above. The designation used for this latter sample is TFE nylon 6,6/DEE.
3. Formic-acid-precipitated nylon 6,6 (FA nylon 6,6) was prepared by dissolving the nylon 6,6 in formic acid (Mallinckrodt, 88% purity) and then *rapidly* precipitating the sample with rapid stirring in deionized water (H_2O) at a H_2O–FA volume ratio of 3 : 1. This was followed by two methanol washes to remove trace formic acid. The sample was filtered using a Buchner funnel and dried in a vacuum oven under a N_2 purge at room temperature. The final sample was a white fibrous material.
4. A formic-acid-precipitated sample was reprecipitated a second time from TFE (TFE FA nylon 6,6) by taking the FA nylon 6,6 sample and redissolving and reprecipitating it in the same manner as the TFE nylon 6,6.

Several pellets of nylon 6,6 were swollen in MeOH at room temperature by immersion in the liquid MeOH for 48 h in a covered container. They were dried in a vacuum oven at ca. 25 mmHg at a temperature of 45–55°C.

A sample of nylon 6,6 containing CaF_2 was prepared in the laboratory by taking precursor nylon 6,6 salts and 3000 ppm of CaF_2 (Aldrich 99.9% pure, 325 mesh) and polymerizing the nylon 6,6 in a laboratory autoclave. The autoclave conditions were similar to those utilized for the commercial nylon 6,6 plant production. A control sample without CaF_2 was also prepared from nylon 6,6 salts in the laboratory autoclave.

Doubly processed nylon 6,6 was produced by taking a standard lot of nylon 6,6 and processing it a second time using a single-screw extruder. The sample was extruded at 285°C following a 2-min residence time in the extruder. A complete listing of sample names and designations is given in Table I.

Analytical Procedures

The crystallization behavior and morphology of the nylon 6,6 samples were characterized by the following analytical methods:

Differential scanning calorimetry (DSC) was conducted on Perkin–Elmer DSC models 2C and 7. Samples were ca. 10 mg in size and scanned in crimped aluminum pans under a nitrogen purge of 20 cm^3/min. Heating scans were conducted at a rate of 20°C/min (typically from 0 to 300°C). The crystallization peak temperature upon cooling from the melt, T_{mc}, was evaluated by heating samples to

Table I Sample Designations and Descriptions for Nylon 6,6 Samples

Sample Designation	Description
Nylon 6,6	Plant-produced nylon 6,6
TFE nylon 6,6	Nylon 6,6 precipitated using TFE/MeOH
FA nylon 6,6	Nylon 6,6 precipitated using FA/H_2O + MeOH wash
TFE FA nylon 6,6	FA nylon 6,6 precipitated using TFE/MeOH
L-Nylon 6,6	Nylon 6,6 salts polymerized in a laboratory autoclave
L-Nylon 6,6 (CaF_2)	Nylon 6,6 salts polymerized in a laboratory autoclave with 3000 ppm CaF_2 added prior to polymerization
DP nylon 6,6	Plant-produced nylon 6,6 processed a second time using a lab extruder

300°C (which is close to the value of T_m^0 = 300–301°C reported in the literature[13–15]), annealing for either 10 or 30 min, and cooling at a rate of 10°C/min to 150°C. Samples to be used for polarized optical microscopy were then immediately quenched by removing them from the thermal cell and placing them on the cold (ca. 10°C) stainless steel analyzer deck surface of the DSC housing.

Polarized optical microscopy (POM) was performed with a Nikon Diaphot inverted microscope coupled to a Bio-Rad 600 confocal microscope system. Samples generated by the DSC analyses were removed from the DSC pans and embedded in the epoxy medium Em-Bed 812. A Reichert-Jüng Ultracut E microtome equipped with a glass knife was used to cut 4-μm thick sections. The samples were covered with a low-viscosity immersion oil on a microscope slide and viewed between crossed polarizers. Photomicrographic digital images were recorded with the scanning laser confocal system operating with an optional transmission detection device.

Wide-angle X-ray scattering (WAXS) was conducted using a Scintag/Seifert PAD V diffractometer (CuK_α radiation, 45 kV and 40 mA) with an ORTEC HyperPure germanium crystal detector. Apiezon "M" grease was used to mount specimens onto the sample holder. Since the grease itself exhibits a scattering maximum at 2θ = 16.9°, this artifact peak was removed by computer deletion from the WAXS scans for the nylon 6,6 samples and replaced with a straight line.

Several other analytical procedures described below were employed to determine if any of the solvent precipitation procedures resulted in changes in the physical properties or chemical structure of the nylon 6,6, or in the addition of measurable contaminants to the nylon 6,6 samples. These procedures included:

Thermogravimetric analysis (TGA) was performed on samples that were first freeze-dried in liquid nitrogen and ground to a powder using a Spex Wig-L-Bug ball grinder. A PL Thermal Sciences STA 1500 TGA was used employing a scanning rate of 10°C/min from 25 to 300°C. Samples were run in platinum crucibles under a nitrogen purge of 20 cm^3/min.

Mass spectrometry (MS) was conducted using a Finnigan 4500 mass spectrometer. Samples (freeze-dried and ground as described for TGA) were run under high vacuum and heated from 35 to 200°C. Samples were heated in 10°C increments with a 30-s hold up to 105°C, then ramped to 125, 150, 175, and 200°C with 30-s holds at each temperature and two 30-s holds at 200°C. Atomic mass 69 was used as the calibration standard.

Combined size-exclusion chromatography/low-angle laser light scattering (SEC/LALLS) was performed on samples dissolved in hexafluoroisopropanol (HFIP) at a concentration of approximately 5 mg/mL. The equipment utilized four PL gel columns with mean permeabilities ranging from 10^6 to 10^3 Å, a Waters model 410 differential refractive index detector, a Kratos model 757 UV detector, and a Chromatix KMX-6 low-angle light-scattering photometer detector. Poly(methyl methacrylate) was used as the molecular weight standard. The molecular weights and distributions of the nylon 6,6 samples were determined using standard procedures for SEC/LALLS analysis.[16]

Fourier-transform infrared spectroscopy (FTIR) was conducted on a Nicolet model 800 FTIR fitted with a Spectra-Tech IR-Plan III microscope accessory. IR spectra were generated using 100 coadded scans collected at a resolution of 4 cm^{-1}. Samples were prepared by using a scalpel to slice thin wedges. A thin film of nylon 6,6 was cast from the TFE solution directly onto a silicon wafer for comparison with the solvent-precipitated samples.

Ion-selective electrode analysis and inductively coupled argon plasma atomic emission spectroscopy (ICP-AES) were used to determine the amount of CaF_2 in the laboratory sample of nylon 6,6 containing CaF_2. The sample was first decomposed in a Parr oxygen bomb at a pressure of 18 atm of oxygen. The resulting combustion product was then analyzed using an Orion ion-selective electrode and a Jarrell-Ash ICP-AES for fluorine and calcium detection, respectively.

RESULTS AND DISCUSSION

Characterization of Commercial Melt-Polymerized Nylon 6,6 Pellets

The crystallization behavior and morphology of the starting nylon 6,6 pellets were studied in detail to provide a reference point for comparison to nylon 6,6 samples prepared by solvent precipitation. The initial DSC heating scan for nylon 6,6 is shown in Figure 1. There are several features of note with regard to this heating scan. This sample has an observed melting point (T_m) or endotherm maximum of 266°C. The small exotherm just before the onset of the melting endotherm is most likely a result of crystallization of less perfect crystals melted during

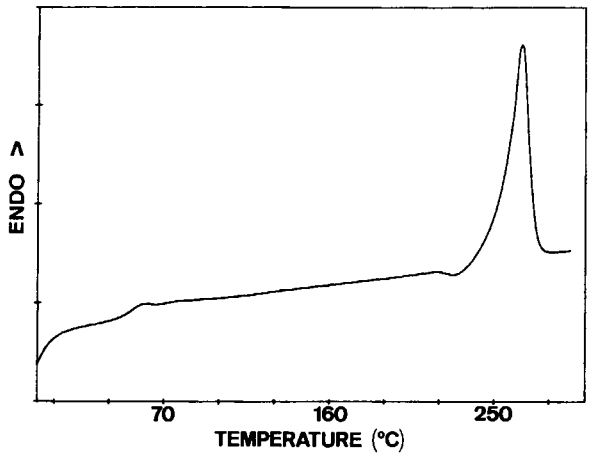

Figure 1 Initial DSC heating scan for nylon 6,6. Scan rate: 20°C/min.

the heating process, or release of processing-induced orientation just prior to melting.[17] The typical enthalpy of melting value is on the order of 17–18 cal/g, corresponding to approximately 40% crystallinity (using a value of ΔH_m = ca. 45 cal/g for 100% crystalline nylon 6,6.[18,19] The observed glass transition temperature (T_g) for the dry nylon 6,6 is ca. 55°C. This is in reasonable agreement with the value of 50°C reported in the literature.[20]

A rapid, qualitative assessment of the overall polymer crystallization rate can be made by evaluating the crystallization peak temperature upon cooling from the melt, or T_{mc}. This value, which is indirectly related to the overall crystallization rate, is influenced by factors such as nucleating agents, temperature of the melt, time in the melt, and molecular weight.[9–12] T_{mc} values measured at a cooling rate of 10°C/min for the starting nylon 6,6 and for the solvent-precipitated nylon 6,6 samples (which will be discussed later) are listed in Table II. The data in Table II show that the T_{mc} for the nylon 6,6 is ca. 223°C with little change in this value when the annealing time at 300°C is increased from 10 to 30 min.

POM was used as a means of directly observing the spherulitic superstructure generated in samples thermally treated in the DSC. Figure 2 is an optical micrograph of the starting nylon 6,6 sample annealed for 30 min at 300°C. This figure shows large (several hundred microns in area on average) impinged spherulites with well-defined Maltese cross patterns and spherulitic boundaries.

WAXS was used to determine the short-range crystal structure and how it changes as a function of thermal treatment and/or processing conditions. Figure 3 contains WAXS scans for the starting nylon 6,6. Scans are shown for the unannealed as-received sample, and for that following melting and recrystallization in the DSC pan. The WAXS scan for the as-received nylon 6,6 sample shows a single broad peak with a maximum at $2\theta = 20.7°$ and a shoulder at 22.2°. This room temperature pattern has been associated with nylon 6,6 samples cooled quickly from the melt.[21–24] The maximum at $2\theta = 20.7°$ has the same 2θ value as for the α_1 reflection of the nylon 6,6 α phase described by Murthy and co-workers.[25] This maximum corresponds to ordering along the (100) plane and has been attributed to the distance between chains that are hydrogen-bonded.[13,25] The scan for the melted and slowly cooled nylon 6,6 sample contains well-defined maxima at 2θ values of 20.4° and 24.0°. These values are close to those assigned to the α_1 (20.8°) and α_2 (24.3°) crystalline reflections characteristic of the α crystalline form of nylon 6,6.[25] The second maximum results from ordering along the (010) and (110) planes and is attributed to the separation between hydrogen-bonded sheets.[13,25] The presence of the second maximum and improved peak definition in the scan for the thermally treated sample shows that melting and slow cooling have enhanced local order in the crystal structure of the starting nylon 6,6. A small (ca. 10%) increase in the percent crystallinity was observed as a result of annealing.

Characterization of Solvent-Precipitated Nylon 6,6

Initial DSC heating scans for the solvent-precipitated nylon 6,6 samples are shown in Figure 4. The melting temperatures for the solvent-precipitated samples are on the order of 2–4°C lower than that for the starting nylon 6,6 (ca. 266°C). This depression could be a consequence of residual solvent in the polymer (following precipitation and drying),

Table II T_{mc} Values for Starting Nylon 6,6 and Solvent-Precipitated Samples

	T_{mc} Values (°C)	
	Annealing Time at 300°C	
Sample Designation	10 min	30 min
Nylon 6,6	223.1	222.0
FA nylon 6,6	231.9	230.1
TFE nylon 6,6	230.7	229.5
TFE FA nylon 6,6	233.0	230.0

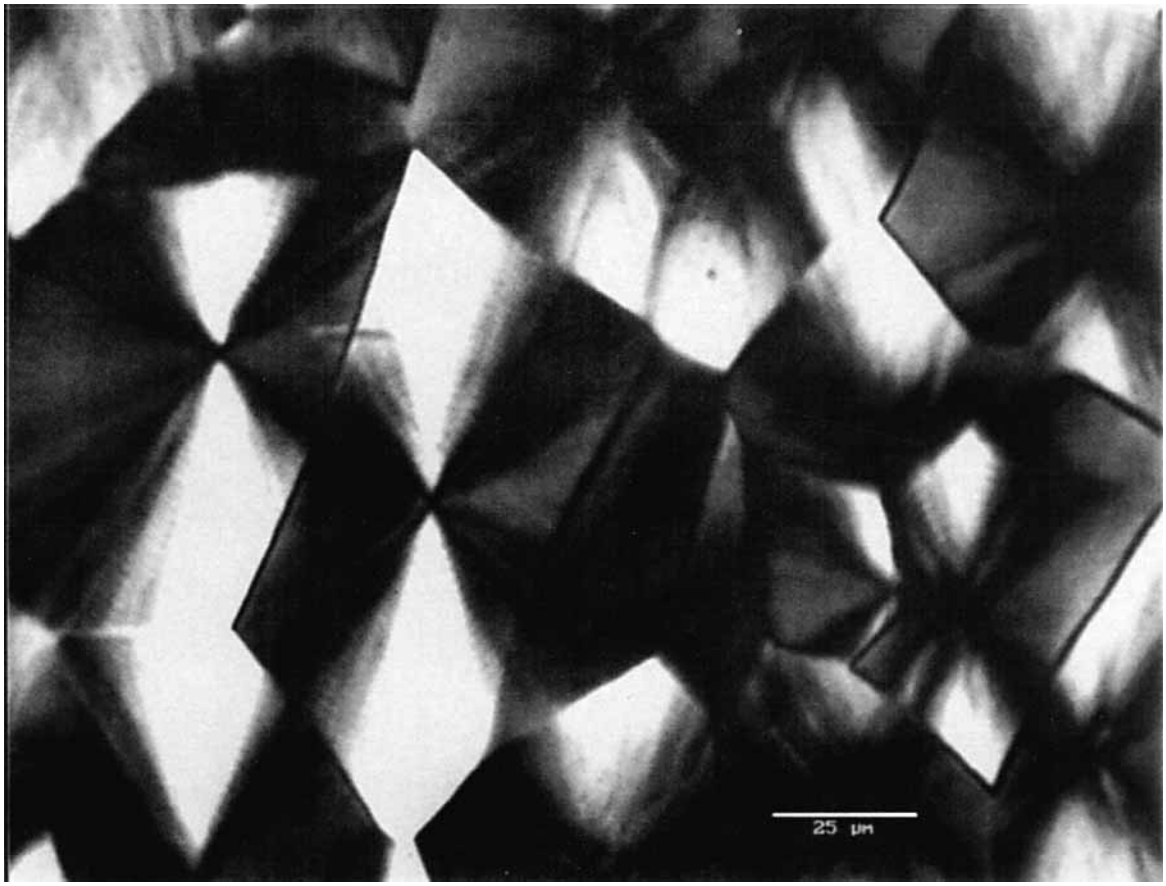

Figure 2 Polarized optical micrograph for nylon 6,6 annealed at 300°C for 30 min, followed by slow cooling. The scale bar is 25 μm.

which would act as a diluent.[26] There may also be orientation of the polymer occurring in the original plant process, which could result in a higher initial melting point. Solvent precipitation could destroy this process-induced orientation and thus lower the observed melting point. Based on polymer T_m data as a function of entrapped solvent for several polymer–solvent systems, we believe that the percentage of residual solvent is sufficiently low as determined by TGA and FTIR, and the latter explanation is

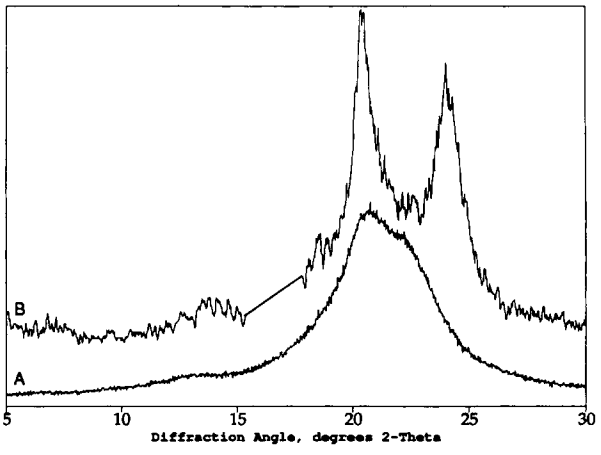

Figure 3 WAXS scans for nylon 6,6 (a) unannealed and (b) annealed at 300°C and slowly cooled.

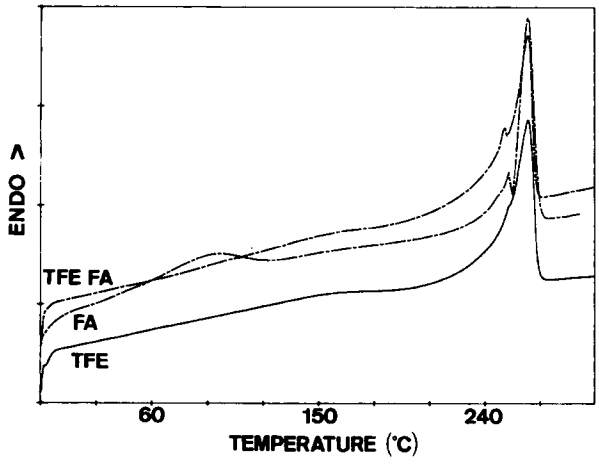

Figure 4 Initial DSC heating scans for solvent-precipitated nylon 6,6. Scan rate: 20°C/min.

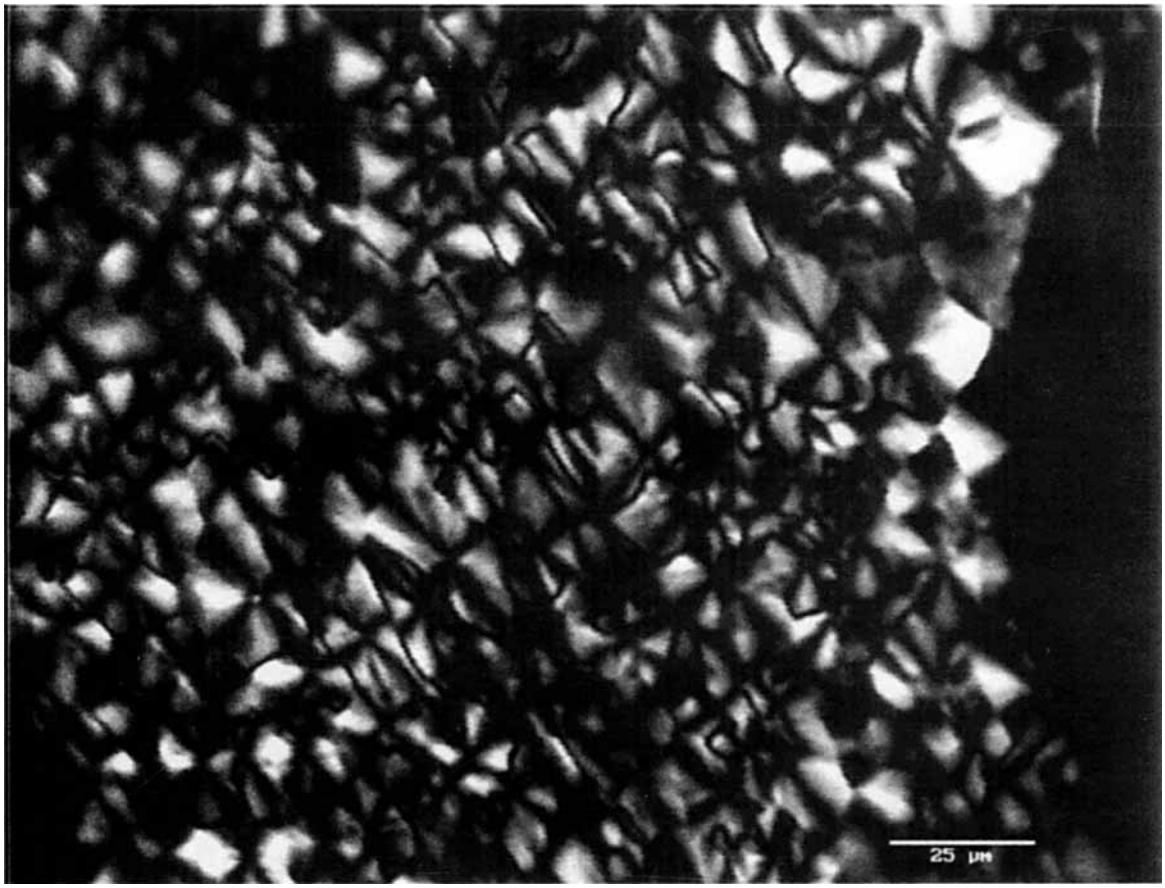

(a)

Figure 5 Polarized optical micrographs for solvent-precipitated nylon 6,6 annealed at 300°C for 30 min and slowly cooled: (a) TFE nylon 6,6; (b) FA nylon 6,6; (c) TFE FA nylon 6,6. The scale bars are 25 μm.

more likely correct.[27] A small side peak with a maximum at ca. 250°C appears in the scans for the solvent-precipitated samples. The development of the side peak at ca. 250°C as a function of cooling rate was discussed previously by Khanna,[17] and it was attributed to a more imperfect crystal form developing at an intermediate cooling rate of 10°C/min. A more imperfect crystal form may also account for the side peaks in the present data. Multiple melting peaks for nylon 6,6 crystallized from solution have also been reported by Starkweather and Jones in the literature.[28] However, it should be noted that Starkweather's data is for nylon 6,6 crystals crystallized from solution under pressure and not rapidly precipitated from a solvent by addition to a nonsolvent as is the case here. They did not report a similar side peak at 250°C.

The enthalpy of melting for the solvent-precipitated samples was ca. 20–22 cal/g. This is approximately 10–20% higher than the value of 17–18 cal/g obtained for the nylon 6,6. We were unable to observe a T_g value in any of the initial DSC heating scans for the solvent-precipitated samples. We do not believe that the T_g was simply depressed as a consequence of residual solvent because no T_g was detected for samples that were scanned starting at over 100°C below the observed T_g (ca. 55°C for the starting plant-processed nylon 6,6). Furthermore, moisture content data reported for nylon 6 show a decrease of 70°C in T_g as the moisture content is increased from 0 to 9%.[29,30] The present samples exhibited a maximum of 5% weight loss by TGA, so it is not expected that the T_g would have been depressed by several decades of temperature. Additionally, the increase in the enthalpy of melting mentioned above, related to an increase in the percent crystallinity, may help to explain why the T_g was not observed. If the percent crystallinity is sufficiently high, it may suppress or "smear" the T_g.[31] Another point of note in the initial DSC heating scans for these solvent-precipitated samples is the presence of the low broad endotherms that appear

(b)

Figure 5 (*Continued from the previous page*)

at temperatures below those of the polymer melting endotherms. Similar results were reported previously by Starkweather and Jones.[28] These endotherms are believed to be caused by the presence of residual solvent in the precipitated samples. This final point will be discussed subsequently in detail.

Values of T_{mc} for solvent-precipitated samples annealed for 10 and 30 min are listed in Table II. Allowing for a variation of approximately ±1°C in the T_{mc} value, the solvent-precipitated samples recrystallize more readily (as indicated by the higher T_{mc} values) than the virgin, melt-polymerized nylon 6,6. The values for the solvent-precipitated samples were, on average, ca. 8°C higher than those for the starting plant-processed samples. This difference is large enough to be significant. However, small differences (on the order of 1–2°C) in T_{mc} for the various solvent-precipitated samples or for samples annealed at the different times are within experimental error. This 8°C increase in T_{mc} for the solvent-precipitated nylon 6,6 samples is not as large as that (14°C) reported previously by Khanna and coworkers.[12]

Polarized optical micrographs of the morphologies for the solvent-precipitated samples used to generate the T_{mc} values are shown in Figures 5(a) to (c). The spherulites shown in Figures 5(a) to (c) for the solvent-precipitated samples, characteristic of a more highly nucleated sample, are much smaller than that for the starting nylon 6,6. There are also regions in these solvent-precipitated samples where there appears to be extinction of the polarized light present at structural boundaries yielding a thin black boundary surrounding the spherulite. The general size of the spherulites within the TFE nylon 6,6 sample [Fig. 5(a)] is more uniform than that for the FA nylon 6,6 sample [Fig. 5(b)]. The morphology of the TFE FA nylon 6,6, shown in Figure 5(c), has the smallest structure of the samples examined. Given the small spherulite size, it is surprising that the corresponding T_{mc} is not higher relative to those for the other solvent-precipitated samples. The data thus confirm that the process of solvent precipitation enhances the overall crystallization rate of nylon 6,6, as evidenced by the uniformly elevated T_{mc} and enhanced nucleation density

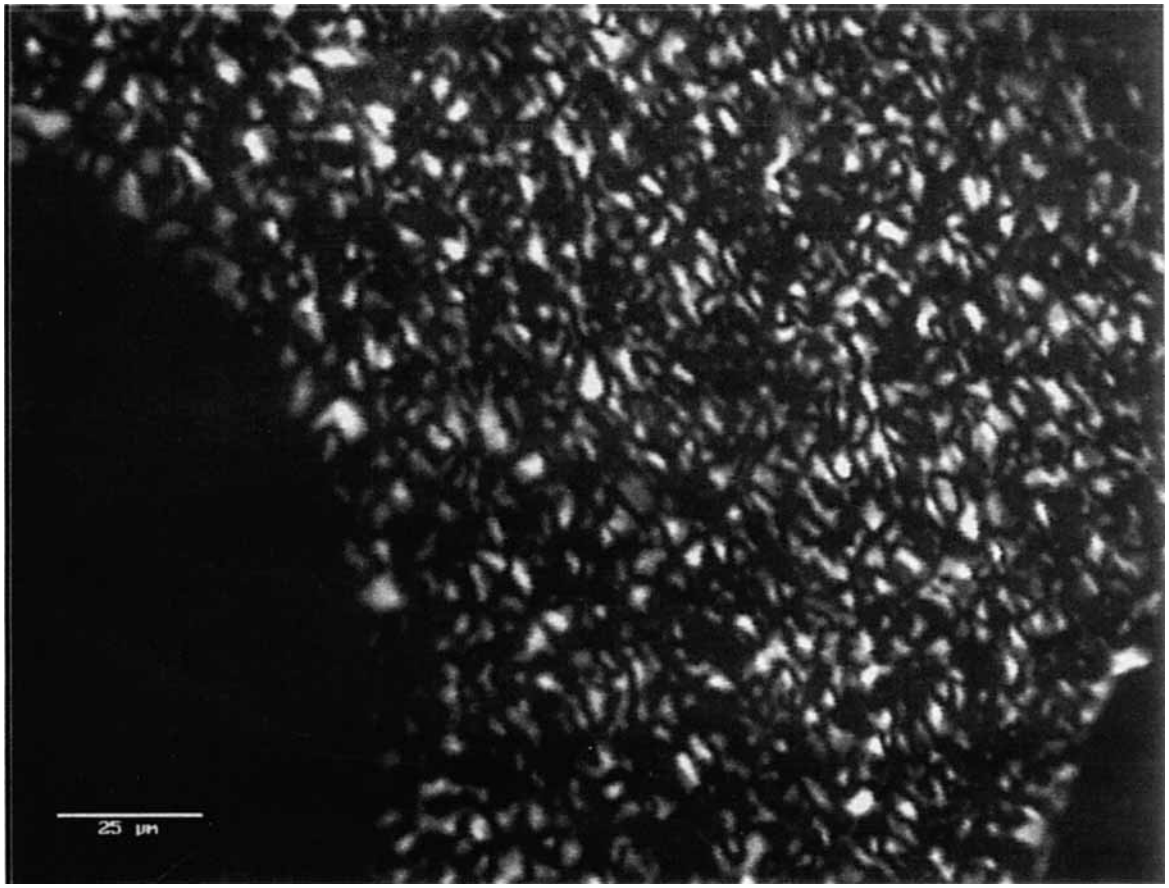

(c)

Figure 5 *(Continued from the previous page)*

observed in the micrographs. There is a qualitative inverse correlation between T_{mc} elevation and spherulite size, as would be expected.

WAXS data for TFE nylon 6,6 samples without and with annealing are shown in Figure 6. Two distinguishable peaks are evident for the unannealed sample, with maxima at $2\theta = 20.5°$ and 23.9°. The peaks present in the scan for the sample annealed at 300°C and slowly cooled show little change in their respective locations ($2\theta = 20.6°$ and 24.2°). What is implied is that the local crystal order present in the unannealed TFE nylon 6,6 is essentially un-

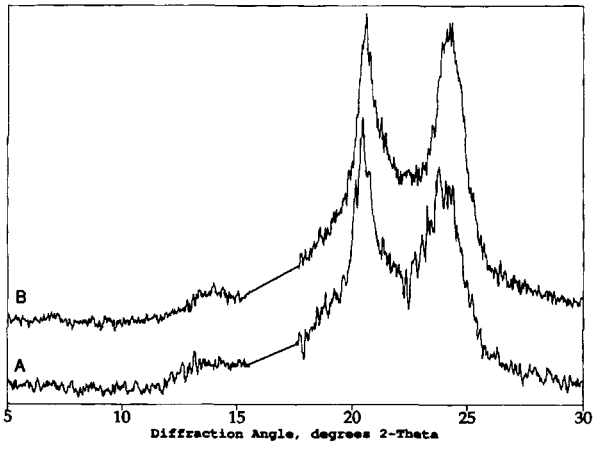

Figure 6 WAXS scans for TFE nylon 6,6: (a) unannealed and (b) annealed at 300°C and slowly cooled.

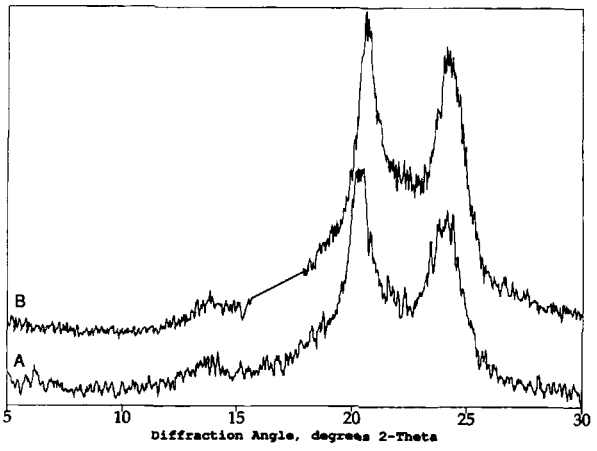

Figure 7 WAXS scans for FA nylon 6,6: (a) unannealed and (b) annealed at 300°C and slowly cooled.

changed by annealing and slow cooling. WAXS scans for the unannealed and annealed FA nylon 6,6 and TFE FA nylon 6,6 samples shown in Figures 7 and 8, respectively, are similar to those for TFE nylon 6,6. Peak maxima are located at $2\theta = 20.3°$ and 24.1° (unannealed) and 20.6° and 24.2° (annealed) for FA nylon 6,6, while those for TFE FA nylon 6,6 are located at $2\theta = 20.5°$ and 23.9° (unannealed) and 20.6° and 24.3° (annealed) which are reasonably close to the values assigned by previous researchers for the α_1 and α_2 peaks, respectively.[13,25] These results again suggest that the solvent-precipitated local order is close to that of the starting nylon 6,6, which has been annealed and slowly cooled.

Comparison of Solvent Precipitation to Other Known Means of Enhancing Nylon 6,6 Crystallization Behavior and Morphology

As a way of comparing the effect of solvent precipitation on nylon 6,6 relative to other known methods for altering crystallization behavior and morphology (such as reextrusion or the addition of a heterogeneous nucleating agent), DSC, POM, and WAXS data are presented for (a) nylon 6,6 that has been re-extruded and (b) nylon 6,6 containing calcium fluoride (CaF_2) as a heterogeneous nucleating agent.

Reextruded Nylon 6,6

T_{mc} values for the reextruded sample annealed at 300°C are elevated on the order of 8°C relative to that for the starting nylon 6,6 (231.8 and 230.2°C for 10 and 30 min, respectively). Altering the melt times resulted in little change in the T_{mc} of the sample. These results indicate that reextrusion and solvent precipitation affect the overall crystallization rate to a similar degree. Similar observations regarding the effect of multiple processing on T_{mc} were reported recently by Wyzgoski and Novak.[32]

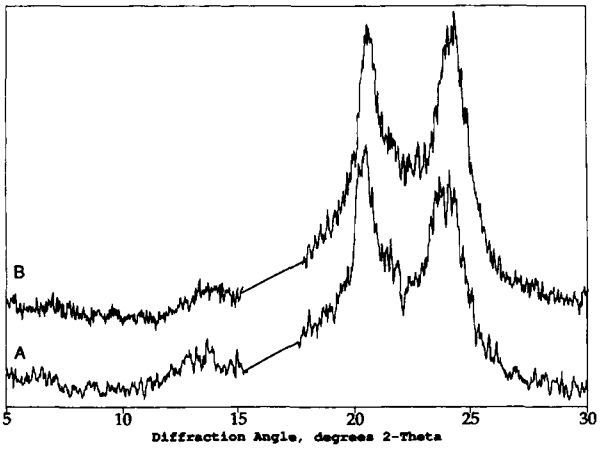

Figure 8 WAXS scans for TFE FA nylon 6,6: (a) unannealed and (b) annealed at 300°C and slowly cooled.

A polarized optical micrograph for the reextruded sample annealed for 30 min at 300°C is shown in Figure 9. The morphology in this reextruded sample is smaller than in the nylon 6,6. The size of the structure is also in the same range as those for the solvent-precipitated samples, which is qualitatively consistent with the T_{mc} results. Wyzgoski and Novak[33] and Starkweather and Brooks[34] similarly reported that nylon 6,6 morphological size decreased with multiple processing because of enhanced overall nucleation.

WAXS results for unannealed and annealed reextruded samples are shown in Figure 10. For the unannealed sample, the WAXS scan contain two poorly resolved peaks with maxima at $2\theta \approx 21.2°$ and 23.3°. Annealing at 300°C for 30 min followed by slow cooling resulted in better peak resolution and separation. The maxima shifted to 2θ values of 20.8° and 24.3°, which are close to the maxima for the starting nylon 6,6 annealed under the same conditions, and to those for the solvent-precipitated samples without and with annealing. These WAXS data show that the reextruded sample has more localized order induced by the second extrusion relative to the starting nylon 6,6, but not to as high a degree as that induced by solvent precipitation.

Lab-Processed Nylon 6,6 Containing CaF_2

Given the above results for solvent precipitation and reextrusion, both methods were deemed unsuitable for introducing CaF_2 into nylon 6,6 to assess its effect as a nucleating agent. In order to assess the unconvoluted effect of CaF_2, it was mixed with the nylon 6,6 precursor salts, and the nylon 6,6 was then polymerized in a laboratory autoclave. The two samples prepared were a control sample containing no CaF_2, and a sample with 3000 ppm CaF_2 added. Ion-selective electrode analysis for fluorine and ICP-AES for calcium yielded a value of 2100 ppm CaF_2 in the resulting nylon 6,6 sample.

T_{mc} data for nylon 6,6 with and without added CaF_2 are listed in Table III for samples annealed at 300°C. The data show that there is a very distinct difference (ca. 6°C) between these values for the two samples. This difference was not changed as the annealing time was increased from 10 to 30 min. These data show that the CaF_2 is enhancing the recrystallization rate of the nylon 6,6 under these conditions to a similar degree as what was observed for the solvent-precipitated samples.

Polarized optical micrographs for the lab-processed nylon 6,6 samples without and with CaF_2 fol-

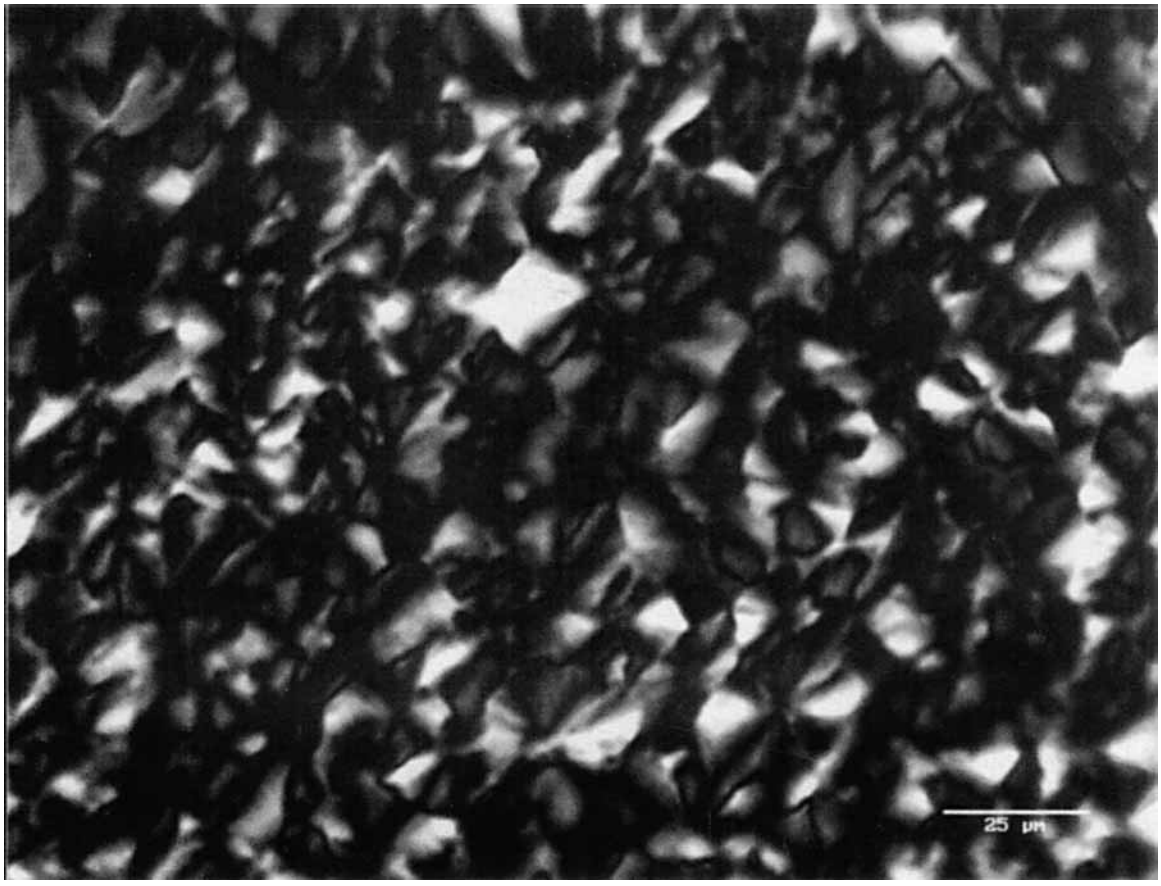

Figure 9 Polarized optical micrograph for reextruded nylon 6,6 annealed at 300°C for 30 min and slowly cooled. The scale bar is 25 μm.

lowing annealing at 300°C for 30 min are shown in Figures 11(a) and (b), respectively. The CaF_2-containing sample is much more highly nucleated than that without CaF_2. The difference in spherulite size of the sample containing CaF_2 compared to the control is not as large as that between the solvent-precipitated nylon 6,6 and the nylon 6,6 annealed under the same conditions [see Figs. 2 and 5(a)–(c)]. However, the spherulites in the CaF_2-containing nylon 6,6 are approximately an order of magnitude smaller compared to those in the control sample. The POM results are qualitatively consistent with those obtained by DSC.

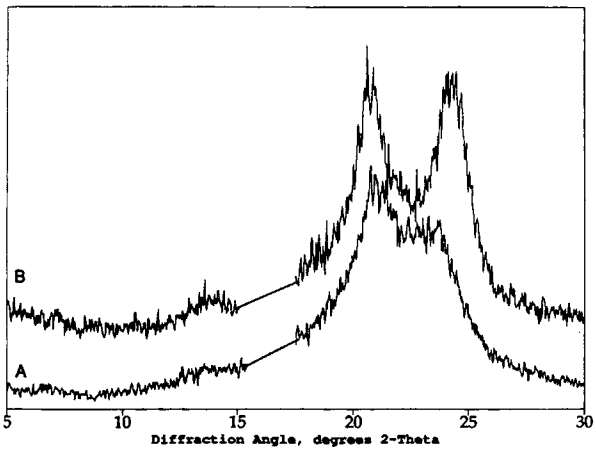

Figure 10 WAXS scans for reextruded nylon 6,6: (a) unannealed and (b) annealed at 300°C for 30 min and slowly cooled.

Table III T_{mc} Values for Lab-Processed Nylon 6,6 Containing No and 2100 ppm CaF_2

	T_{mc} Values (°C)	
	Annealing Time at 300°C	
Sample Designation	10 min	30 min
L-Nylon 6,6	224.8	222.8
L-Nylon 6,6 (CaF_2)	231.3	230.0

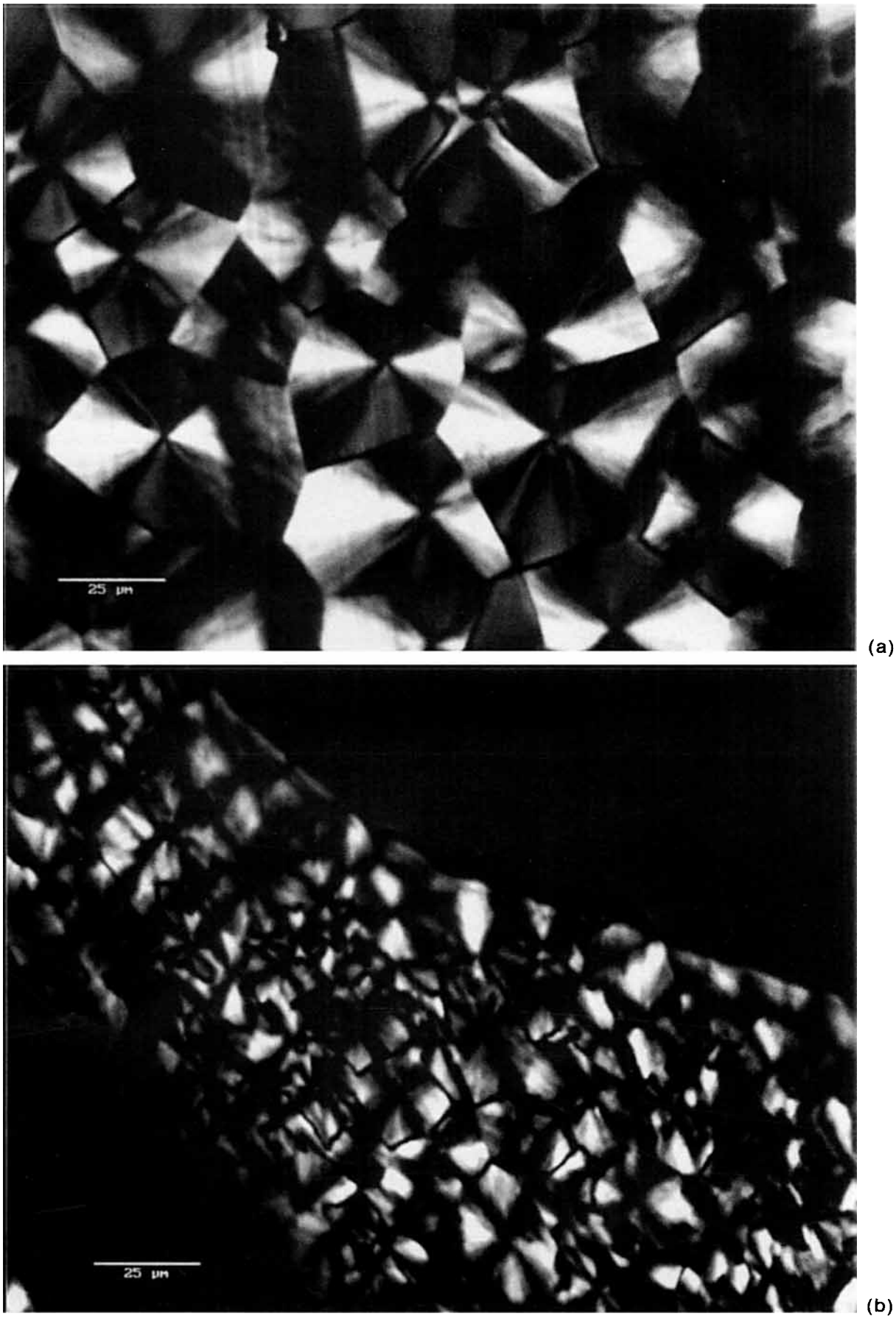

Figure 11 Polarized optical micrographs for lab-processed nylon 6,6: (a) containing no CaF_2 and (b) containing 2100 ppm CaF_2, both annealed at 300°C for 30 min and slowly cooled. The scale bars are 25 μm.

WAXS scans for the control and CaF_2-containing samples are shown in Figures 12 and 13, respectively. Scans for unannealed and annealed (300°C for 30 min and slowly cooled) samples are shown in each figure. Annealing and slow cooling resulted in better peak resolution and separation for both the control and the nylon 6,6 with CaF_2. Referring to Figures 12 and 13, peak maxima are located at 2θ = 20.8° and 23.6° (unannealed) and 20.8° and 24.2° (annealed) for the control, and at 2θ = 20.8° and 23.1° (unannealed) and 20.7° and 24.3° (annealed) for the nylon 6,6 + CaF_2. The level of CaF_2 was too low to be detected by WAXS. The maxima values for the annealed samples agree well with the α_1 and α_2 peak assignments discussed earlier with regard to the starting nylon 6,6 results.[13,25]

Summarizing this section, solvent precipitation, addition of CaF_2, and reextrusion appear to have a similar effect on the overall crystallization rate and spherulite size in nylon 6,6. Also, solvent precipitation appears to induce the highest degree of local order in the unannealed samples as measured by WAXS. The order is similar to that measured for samples that have been melted and slowly cooled.

Molecular Characterization of Solvent-Precipitated Nylon 6,6

Several analytical techniques were used to determine if any unexpected impurities or structural changes had been introduced into the nylon 6,6 during the solvent precipitation process. If present, these impurities or changes could account for the more highly nucleated nylon 6,6. We also wished to assess how much residual solvent was introduced into the nylon

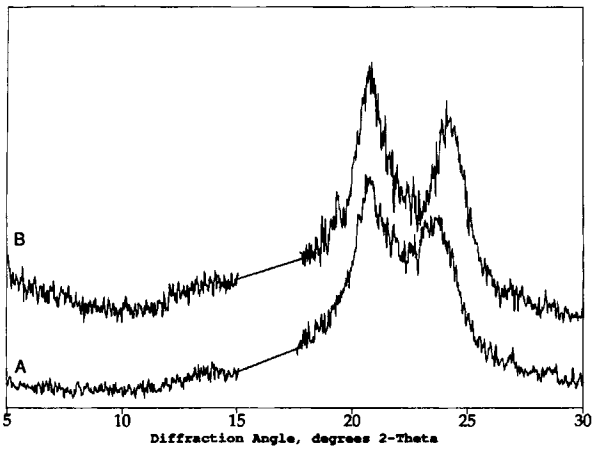

Figure 12 WAXS scans for lab-processed nylon 6,6 containing no CaF_2: (a) unannealed and (b) annealed at 300°C for 30 min and slowly cooled.

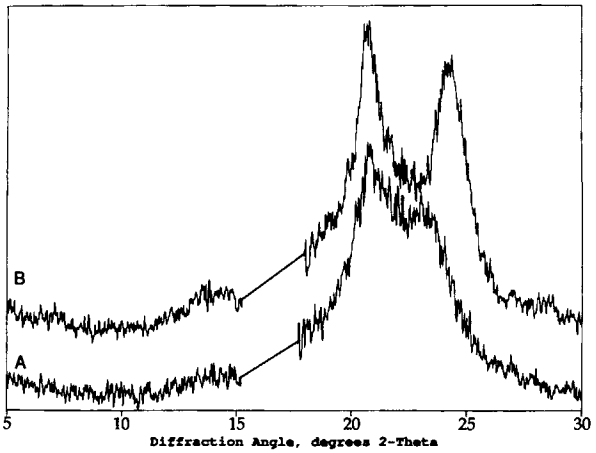

Figure 13 WAXS scans for lab-processed nylon 6,6 containing 2100 ppm CaF_2: (a) unannealed and (b) annealed at 300°C for 30 min and slowly cooled.

6,6 through the precipitation process. Experiments included TGA, MS, SEC/LALLS, and FTIR. Results from these experiments are described below.

TGA and MS analyses on the nylon 6,6, FA, and TFE-precipitated samples were conducted to estimate the amount of residual solvent incorporated into the solvent-precipitated nylon 6,6. TGA scans for the nylon 6,6, FA nylon 6,6, and TFE nylon 6,6 samples are shown in Figures 14(a) to (c), respectively. Total overall percent weight loss as a function of heating to 300°C is listed in Table IV. TGA revealed ca. 1.1% weight loss by 100°C for the nylon 6,6. Both the FA and TFE nylon 6,6 showed approximately 1.5% weight loss by 75°C, and the latter had an additional 3% weight loss by 160°C. In all three cases, the low-temperature slope changes in the weight loss scans [and exotherm peaks in the differential thermal analysis (DTA) scans also shown on each plot in Fig. 14] correspond to solvent loss. The weight loss observed for the nylon 6,6 is most likely a consequence of desorption of water. The weight loss observed at 75°C for the FA nylon 6,6 could be a result of both formic acid and water (bp = 100°C). Similarly, the weight loss observed in the first temperature range for the TFE sample is likely due to both methanol (bp = 100°C) and TFE (bp = 75°C).[35] The peak at the higher temperature may be due to hydrogen-bonded TFE or water.

Solids probe mass spectrometry was also employed to verify the molecular structure of the volatiles measured by TGA. While it is recognized that direct comparison of results between the TGA and MS methods cannot be made because of differences in experimental conditions, there was evidence for

water in the nylon 6,6, formic acid in the FA nylon 6,6 without strong evidence for water, and trifluoroethanol with possible trace methanol in the TFE nylon 6,6. The relative quantitative amounts of the residual solvents, however, could not be determined by this method. The additional weight loss data (Table IV) provided by simply weighing the DSC samples before and after thermal treatment are in qualitative agreement with the TGA results.

The influence of polymer molecular weight on overall crystallization rate has long been recognized, and it has been reported previously.[36-38] SEC/LALLS was therefore performed to test whether the molecular weight or molecular weight distribution of the nylon 6,6 was changed as a result of solvent precipitation. Results are shown in Table V. No major differences between the samples were revealed by this technique. This provides direct evidence that the solvent precipitation process does not induce changes in the nylon 6,6 molecular weight or molecular weight distribution.

FTIR was also utilized to determine whether any unexpected molecular degradation or changes might have occurred during the FA or TFE dissolution process. The infrared spectra of these samples are identical, indicating no major IR-detectable differences (ca. < 0.2 wt %) between samples.

Summarizing this section, the above experimental data yielded no detectable evidence that the process of dissolving and precipitating nylon 6,6 produces any major molecular structural changes or molecular weight and distribution changes in the nylon 6,6. This is consistent with results presented by Khanna and co-workers for nylon 6.[10] These studies indicate, however, that the process of solvent precipitation does leave up to several percent entrapped solvent in the nylon 6,6 samples. This is not a surprising finding, considering the tenacity with which nylon 6,6 absorbs and retains hydroxylic solvents. The effects of the solvent precipitation process upon the crystallization behavior and morphology can, therefore, be ascribed to either the solvent precipitation process itself or to effects of residual solvent trapped in the nylon 6,6.

Effect of Solvent Precipitation vs. Residual Solvent on the Crystallization Behavior of Precipitated Nylon 6,6

In an effort to more fully understand the role of residual solvent and the solvent precipitation process in enhancing the overall crystallization of nylon 6,6, several additional experiments were undertaken. Results from these experiments are presented below.

In order to test whether the presence of residual solvent altered the crystallization behavior of nylon 6,6, we investigated the effects of solvent absorption. This was accomplished by swelling several pellets of the starting nylon 6,6 in liquid MeOH. The T_{mc} values of 223°C for these samples were identical, within experimental error, to those for the plant-processed nylon 6,6 that had been melted at 300°C for 10 min. This experiment shows that the presence of residual hydrogen-bonding nonsolvent present in the nylon 6,6 is not sufficient to induce subsequent changes in the crystallization behavior.

The next experiment tested whether the solvent precipitation process using a less hydrogen-bonding nonsolvent (diethyl ether, DEE) would still enhance the crystallization behavior of the precipitated nylon 6,6. Values of T_{mc} for nylon 6,6 dissolved in TFE and precipitated from diethyl ether (designated as TFE nylon 6,6/DEE) were equivalent ($T_{mc} \approx 230$°C) within experimental error to those discussed earlier for the TFE nylon 6,6, FA nylon 6,6, and TFE FA nylon 6,6 precipitated in MeOH. This latter experiment shows that the actual solvent precipitation process is more crucial than the H-bonding character of the nonsolvent for enhancing the nylon 6,6 overall crystallization rate. We thus believe that these two experiments show that it is, in fact, the process of solvent precipitation and *not* the presence of residual solvent that is responsible for enhancing the overall crystallization rate of nylon 6,6.

Effect of Solution Concentration on Crystallization Behavior of Solvent Precipitated Nylon 6,6

A study was then conducted to determine whether the effect of concentration of nylon 6,6 in TFE affects the crystallization behavior of the precipitated nylon 6,6. A plot showing T_{mc} as a function of TFE solution concentration prior to precipitation is shown in Figure 15. Results show that T_{mc} decreases by ca. 4°C as the solution concentration increases from 0.1 to 1.5%, after which point it appears to level off with increasing concentration up to 5%.

Khanna and co-workers[14,15] reported that several processing treatments, including solvent precipitation, increase the overall crystallization rate of various nylons. They hypothesized that solvent precipitation, for example, is effective because the dissolution process disrupts the initial disorder stabilized by hydrogen bonding existing in the virgin nylon. Once this has occurred, locally ordered regions then form. As these regions are stabilized by hydrogen bonding, they survive in the melt and can thus serve

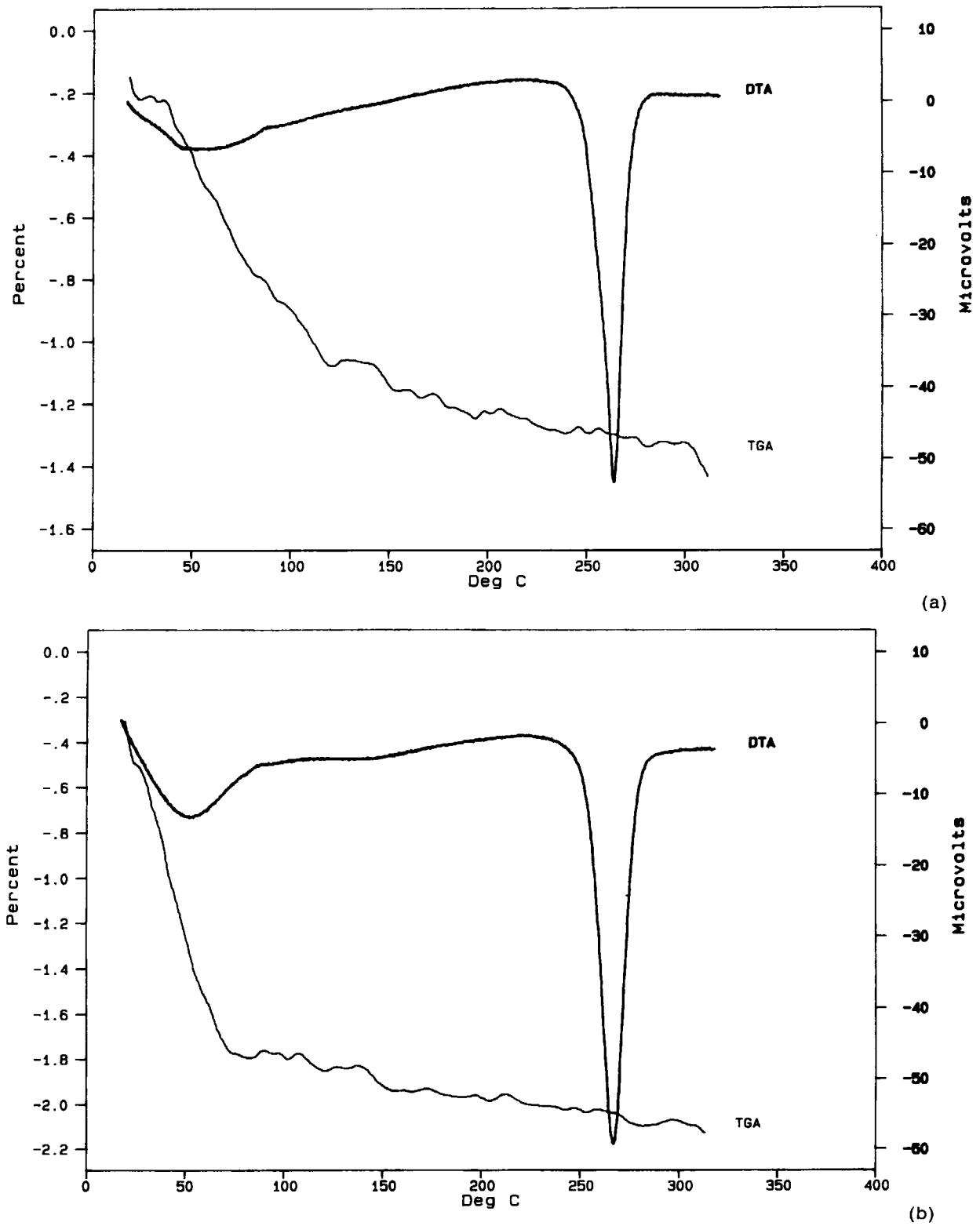

Figure 14 TGA scans for starting nylon 6,6 and solvent-precipitated nylon 6,6: (a) nylon 6,6: (b) FA nylon 6,6; and (c) TFE nylon 6,6. Scan rate: 10°C/min.

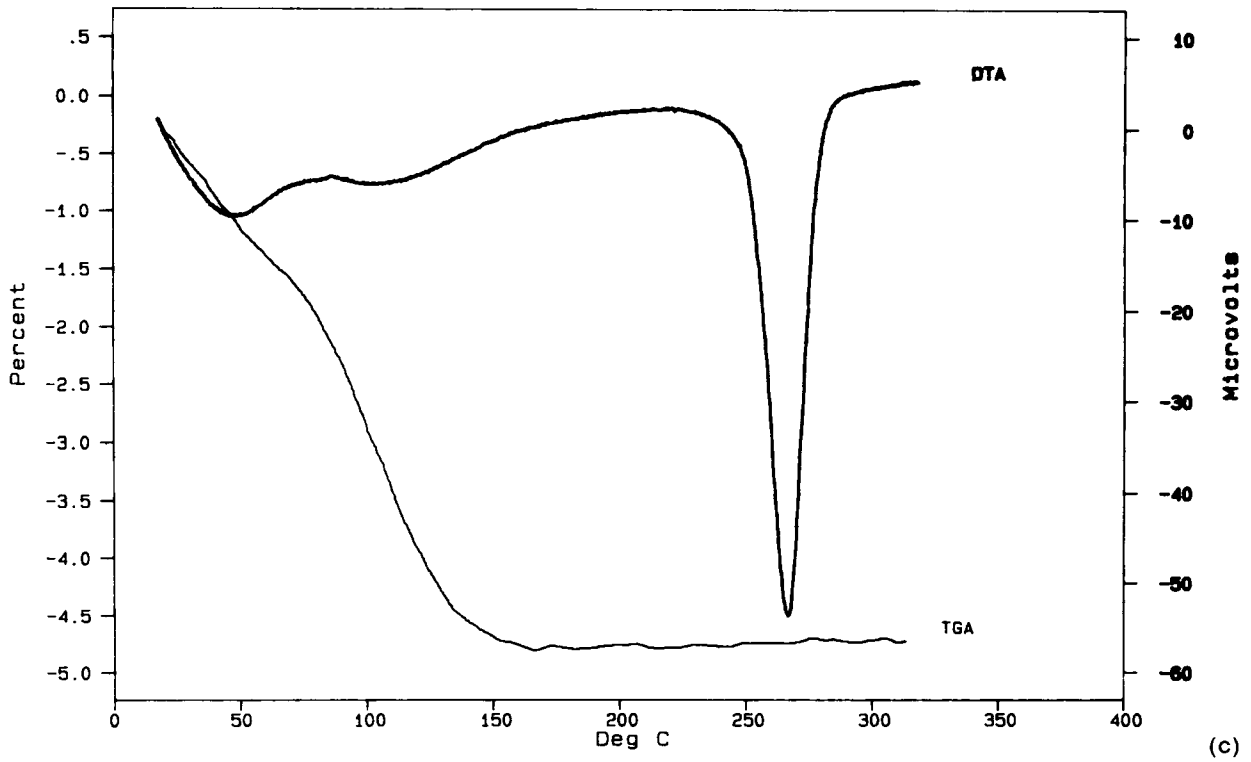

Figure 14 *(Continued from previous page)*

as sites for nucleation, resulting in a higher overall crystallization rate.[14,15] We believe that the data in the present work are in line with this hypothesis as it applies to nylon 6,6. However, the solution concentration data require some additional elaboration. We propose that the trend in the T_{mc} data shown in Figure 15 may be explained by solution entanglement effects. At low polymer solution concentrations, there are fewer entanglements so that the polymer can more easily order. These ordered regions can serve as nucleation sites, promoting more rapid crystallization following melting in the precipitated sample. At the higher solution concentrations, however, polymer entanglements can interfere with the ordering and thus reduce the number of ordered regions formed.

Table IV Weight Loss Data for Starting Nylon 6,6 and Solvent-Precipitated Nylon 6,6

Sample	DSC Sample Wt. Loss (%)	TGA Sample Wt. Loss (%)
Nylon 6,6	1.5	1.4
TFE nylon 6,6	3.0	4.7
FA nylon 6,6	4.0	1.7
TFE FA nylon 6,6	1.0	—

If the polymer entanglement proposal is correct, then there is a critical concentration, c^*, at which entanglements begin to form and the solution becomes semidilute.[39,40] This critical concentration can be approximated as follows[40]:

$$c^* = 1/[\eta] \quad (1)$$

where $[\eta]$ is the intrinsic viscosity. Intrinsic viscosity $[\eta]$ is related to the molecular weight by the Mark–Houwink equation, defined as

Table V Molecular Weight Data Determined by SEC/LALLS for Starting Nylon 6,6 and Solvent-Precipitated Nylon 6,6

Sample	M_w	Corrected* M_n	Corrected* M_w/M_n
Nylon 6,6			
Avg.	44,599	20,285	2.20
Std. Dev.	688	383	0.03
FA nylon 6,6			
Avg.	44,426	19,992	2.22
Std. Dev.	412	61	0.01
TFE FA nylon 6,6			
Avg.	45,608	19,282	2.37
Std. Dev.	630	933	0.08

* Corrected using poly(methyl methacrylate) as the molecular weight standard.

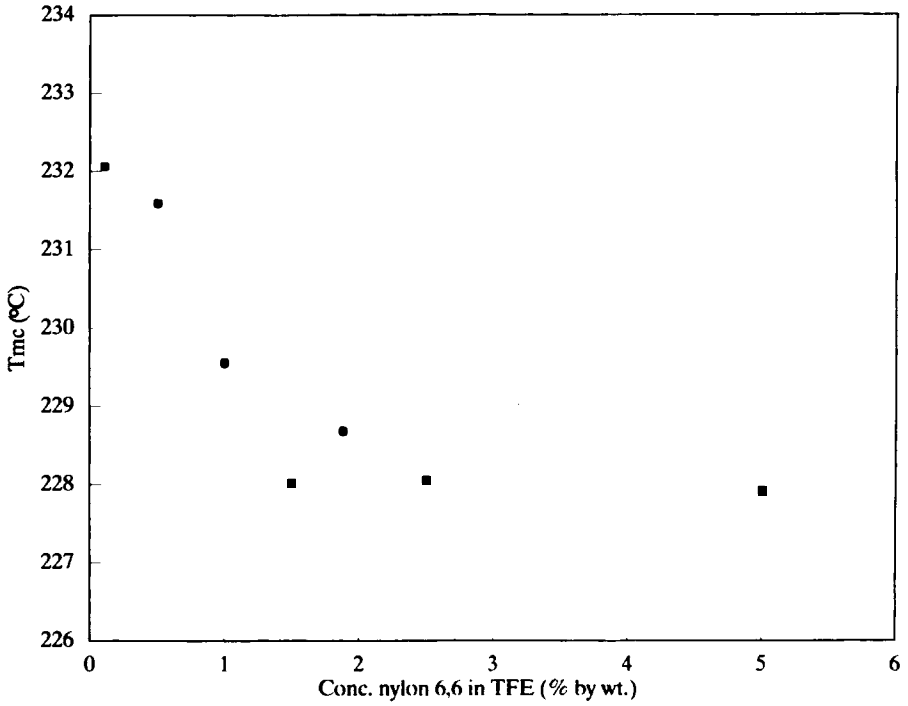

Figure 15 T_{mc} as a function of TFE solution concentration prior to precipitation.

$$[\eta] = KM^a \quad (2)$$

where K and a are constants that depend on the polymer, solvent, and temperature. M in this case is the weight-average molecular weight (44,600 by SEC/LALLS for nylon 6,6 in HFIP at 25°C). K depends on the breadth of the molecular weight distribution, and a is a measure of the polymer–solvent interactions.[41–43] Nylon 6,6 intrinsic viscosity parameters of $K = 1.98 \times 10^{-3}$ and $a = 0.63$ are reported by Sumantra for nylon 6,6 in hexafluoroisopropanol (HFIP).[43] With these values in Eq. (2), c^* is calculated to be 0.006 g/mL. The region at which T_{mc} begins to plateau in Figure 15 is near 1.5% in TFE, which is equivalent to 0.021 g/mL. The actual concentration of polymer solution where entanglements begin to affect solution properties is several times larger than the calculated c^*.[39] Our observed value of c^* of 0.021 g/mL for nylon 6,6 in TFE is in line with this generalization. This appears to support our hypothesis that nylon 6,6 entanglements in solution partially affect the formation of ordered regions in the nylon 6,6. However, more direct evidence from solution experiments such as zero shear viscosity determination are needed to prove that solution entanglements are responsible for this effect on T_{mc}.

An alternate proposal put forth by Phillips addresses the issue of whether the nylon 6,6 solution is, in fact, a true solution.[44] If not a true solution, microscopic "seed crystals" of undissolved nylon 6,6 present at low polymer concentrations exist that can serve as nucleation sites. Alternatively, seed crystals could be forming during the early stages of precipitation. As the nylon 6,6 concentration increases, the seed crystals agglomerate and spherulitic frameworks form. These agglomerates of seed crystals could be less effective as nucleation sites, which would account for the decrease in T_{mc} relative to the lowest nylon 6,6 concentrations. If this proposal is correct, it would account for both the effect of solvent precipitation and nylon 6,6 solution concentration without recourse to solution ordering stabilized by hydrogen bonding or entanglement effects. However, there is no direct proof for the seed crystals at present, so evidence from an experiment such as solution light scattering would be necessary to verify their existence.

CONCLUSIONS

Solvent precipitation of melt-processed nylon 6,6 results in a material which, upon subsequent melting, exhibits an enhanced T_{mc} and a more highly nucleated morphology relative to the starting material. We have demonstrated that these effects in the solvent-precipitated samples are not conse-

quences of changes in molecular weight or molecular weight distribution (MWD). They also cannot be ascribed to chemical changes or inclusion of impurities in the polymer that might be introduced during the solvent precipitation process. The effect of solvent precipitation rivals that of reextrusion or the introduction of a heterogeneous nucleation agent such as CaF_2.

The increased overall crystallization rate and increased nucleation density arising from the solvent precipitation process are not caused by the presence of entrapped residual solvent in the solid polymer. Rather, the dissolution and precipitation process itself is responsible. Furthermore, these increases can be obtained by using hydroxylic nonsolvents of varying H-bonding character in the precipitation process. Also, the increase in T_{mc} caused by solvent precipitation is affected by the concentration of nylon 6,6 in solution up to ca. 1.5% by weight. As the concentration increases, the T_{mc} of the precipitated nylon 6,6 decreases. The above results are consistent with the model originally proposed by Khanna and co-workers in which dissolved nylon 6,6 forms ordered domains that later serve as nucleation sites. We further propose that the number of these ordered sites formed is partially affected by polymer entanglements in solution, which would be a reasonable explanation for the observed concentration effect. Our results are also consistent with the proposal by Phillips that the solution contains undissolved seed crystals of nylon 6,6 that later serve as nucleation sites. Further experiments are necessary to prove which proposal is correct.

Lastly, our work suggests that for assessing the effect of heterogeneous nucleating agents on the morphology of nylon 6,6, a method for introducing the nucleating agent into the nylon 6,6 must be selected that itself does not alter the crystallization behavior and morphology of the polymer. Both solvent precipitation and reextrusion are poor choices as procedures for introducing heterogeneous nucleating agents into the nylon 6,6. We therefore recommend that to truly study the unconfounded effects of heterogeneous nucleating agents upon the crystallization behavior and morphology of nylon 6,6, the nucleating agents should be added to the nylon salts prior to melt polymerization.

The following people are gratefully acknowledged for their contributions to this work: J. C. Middleton, O. J. Parker, C. E. Schwier, and B. A. Lysek for providing nylon 6,6 samples and helpful discussion. The following people provided invaluable analytical assistance: F. L. May for WAXS; M. J. Pollo for SEC/LALLS; J. J. Tria for TGA; P. C. Toren for MS; S. J. Lemp and C. S. Ling for ion-selective electrode analysis and ICP-AES; and R. L. Ornberg for microtoming assistance. We also thank B. G. Frushour, A. R. Padwa, J. V. Pustinger, E. E. Remsen, N. A. Rotstein, S. R. Sumantra, and Professor P. Phillips for helpful discussions; and P. A. Echelmeier for manuscript preparation.

REFERENCES

1. B. Wunderlich, *Macromolecular Physics, Vol. 2: Crystal Nucleation, Growth, Annealing,* Academic Press, New York, 1976.
2. M. Day, T. Sprunchuk, Y. Deslandes, and D. M. Wiles, *Proc. 34th Int. SAMPE Symp. Exhib.,* May 8–11, 1989.
3. J. Carpenter, *SAMPE J.,* **24,** 36 (1988).
4. Y. Lee and R. S. Porter, *Macromolecules,* **21,** 2770 (1988).
5. D. C. Bassett, R. H. Olley, and I. A. M. Al Raheil, *Polymer,* **29,** 1745 (1988).
6. D. J. Blundell, J. M. Chalmers, M. W. Mackenzie, and W. F. Gaskin, *SAMPE Q.,* **16,** 22 (1985).
7. P. Cebe, S.-D. Hong, S. Chung, and A. Gupta, *Special Technical Publication 937,* ASTM, Philadelphia, 1987, p. 342.
8. V. Brucato, G. Crippa, S. Piccarolo, and G. Titomanlio, *Polym. Eng. Sci.,* **31**(19), 1411 (1991).
9. Y. P. Khanna and A. C. Reimschuessel, *J. Appl. Polym. Sci.,* **35,** 2259 (1988).
10. Y. P. Khanna, A. C. Reimschuessel, A. Banerjie, and C. Altman, *Polym. Eng. Sci.,* **28**(24), 1600 (1988).
11. Y. P. Khanna, R. Kumar, and A. C. Reimschuessel, *Polym. Eng. Sci.,* **28**(24), 1607 (1988).
12. Y. P. Khanna, R. Kumar, and A. C. Reimschuessel, *Polym. Eng. Sci.,* **28**(24), 1612 (1988).
13. H. Reimschuessel, "Polyamide Fibers," in *Handbook of Fiber Science and Technology, Vol. 4: Fiber Chemistry,* M. Lewin and E. M. Pearce, Eds., Marcel-Dekker, 1985, p. 73.
14. J. H. Magill, M. Girolamo, and A. Keller, *Polymer,* **22,** 43 (1981).
15. H. Mitomo and K. Nakazato, *Polymer,* **19,** 1427 (1978).
16. W. W. Yau, J. J. Kirkland, and D. D. Bly, *Modern Size-Exclusion Liquid Chromatography: Practice of Gel Permeation and Gel Filtration Chromatography,* Wiley, New York, 1979.
17. Y. P. Khanna, *Macromolecules,* **25,** 3298 (1992).
18. R. Pflüger, in *Polymer Handbook, 3rd ed.,* J. Brandrup and E. H. Immergut, Eds., Wiley, New York, 1989, p. 109.
19. H. W. Starkweather, Jr., P. Zoller, and G. A. Jones, *J. Polym. Sci.: Polym. Phys. Ed.,* **22,** 1615 (1984).
20. W. A. Lee and R. A. Rutherford, *Polymer Handbook, 2nd ed.,* J. Brandrup and E. H. Immergut, Eds., Wiley, New York, 1975, p. III-139.
21. H. W. Starkweather, Jr., in *Nylon Plastics,* M. I. Kohan, Ed., SPE Monographs, New York, 1973.

22. H. W. Starkweather, Jr., *Macromolecules,* **22,** 2000 (1989).
23. H. Haberkorn, K. H. Illers, and P. Simak, *Colloid and Polymer Sci.,* **257,** 820 (1979).
24. H. W. Starkweather, Jr., J. F. Whitney, and D. R. Johnson, *J. Polym. Sci.: Pt. A,* **1,** 715 (1963).
25. N. S. Murthy, S. A. Curran, S. M. Aharoni, and H. Minor, *Macromolecules,* **24,** 3215 (1991).
26. P. J. Flory, *Principles of Polymer Chemistry,* Cornell University Press, Ithaca, 1953.
27. B. Wunderlich, *Macromolecular Physics, Vol. 3: Crystal Melting,* Academic Press, New York, 1980.
28. H. W. Starkweather, Jr. and G. A. Jones, *J. Polym. Sci.: Polym. Phys. Ed.,* **19,** 467 (1981).
29. J. Zimmerman, "Polyamides," in *Encyclopedia of Polymer Science and Engineering, (Vol. 11),* Wiley, New York, 1988, p. 315.
30. I. F. Kaimin, A. P. Apinis, and A. Y. Galvanovskii, *Vysokomol. soyed.,* **A17**(1), 41 (1975).
31. O. Olabisi, L. M. Robeson, and M. T. Shaw, *Polymer-Polymer Miscibility,* Academic Press, New York, 1979, p. 119.
32. M. G. Wyzgoski and G. E. Novak, *Polym. Eng. Sci.,* **32**(16), 1105 (1992).
33. M. G. Wyzgoski and G. E. Novak, *Polym. Eng. Sci.,* **32**(16), 1114 (1992).
34. H. W. Starkweather, Jr. and R. E. Brooks, *J. Appl. Polym. Sci.,* **1**(2), 236 (1959).
35. *CRC Handbook of Chemistry and Physics (64th ed.),* R. C. Weast, Ed., CRC Press, Boca Raton, FL, 1983.
36. P. J. Phillips, *Rep. Prog. Phys.,* **53,** 549 (1990).
37. J. H. Magill, *J. Appl. Phys.,* **35,** 3249 (1964).
38. J. G. Fatou, "Crystallization Kinetics," in *Encyclopedia of Polymer Science and Engineering, (Suppl. Vol.),* Wiley, New York, 1989, p. 231.
39. T. P. Lodge, N. A. Rotstein, and S. Prager, *Adv. Chem. Phys.,* **79,** 1 (1990).
40. A. M. Jamieson, "Solution Rheology," in *Encyclopedia of Polymer Science and Engineering, (Vol. 15),* Wiley, New York, 1989, p. 492.
41. P. C. Hiemenz, *Polymer Chemistry: The Basic Concepts,* Marcel-Dekker, New York, 1984.
42. E. A. Collins, J. Bareš, and F. W. Billmeyer, Jr., *Experiments in Polymer Science,* Wiley, New York, 1973.
43. S. R. Sumantra, *J. Appl. Polym. Sci.,* **45,** 1635 (1992).
44. P. J. Phillips, personal communication, 1993.

Received September 15, 1993
Accepted January 29, 1994